https://doi.org/10.5194/egusphere-2026-824
Preprint. Discussion started: 17 February 2026

Evaluating InSAR-derived rates of surface-elevation change along the central U.S. Gulf Coast

Guandong Li[1], Torbjörn E. Törnqvist[1], Jingyi Chen[2,3]

[1]Department of Earth and Environmental Sciences, Tulane University, 6823 St. Charles Avenue, New Orleans, LA, USA
[2]Department of Aerospace Engineering and Engineering Mechanics, The University of Texas at Austin, Austin, TX, USA
[3]Center for Space Research, The University of Texas at Austin, Austin, TX, USA

Correspondence to: Guandong Li (gli4@tulane.edu)

Abstract. Interferometric Synthetic Aperture Radar (InSAR) is widely used to monitor surface-elevation change in subsiding coastal regions, but inconsistencies between studies hinder understanding of the processes driving vertical land motion (VLM). Here we compare two recent InSAR datasets from the central U.S. Gulf Coast which yield similar mean rates (-2.8 ± 2.8 and -3.3 ± 1.8 mm yr^{-1}) but show negligible spatial correlation ($R^2 = 0.05$), except in medium to highly developed urban areas ($R^2 > 0.5$). Using 41 Global Navigation Satellite System records from adjacent Pleistocene uplands with minimal shallow subsidence and sediment accretion, we find a median VLM of -1.2 mm yr^{-1}, largely driven by glacial isostatic adjustment that is higher than previously believed. InSAR data exhibit larger uncertainties and are presently unable to capture this rate. Given the struggles of InSAR in vegetated landscapes, we recommend that vertical velocities below 5 mm yr^{-1} are interpreted with utmost caution.

1 Introduction

Accelerated sea-level rise increasingly threatens low-lying coastal regions where a large and increasing proportion of the global population resides (Hauer et al., 2020). Coastal subsidence — the downward motion of a specific reference horizon relative to a fixed datum (Törnqvist and Blum, 2024) — plays a critical role in increasing the vulnerability of these settings under a changing climate (e.g., Milliman and Haq, 1996; Bijlsma et al., 1996). A thorough understanding of coastal subsidence is essential for developing resilient strategies and adaptation plans due to the impacts of future climate change.

To support such efforts, various technologies and methods for monitoring coastal subsidence have been developed in recent decades (Shirzaei et al., 2021). The Global Navigation Satellite System (GNSS) is one of the key techniques to continuously measure vertical land motion (VLM) by means of point observations (e.g., Dixon, 1991; Segall and Davis, 1997; Mcclusky et al., 2000; Sella et al., 2002; Sella et al., 2007; Bouin and Wöppelmann, 2010; Hammond et al., 2021; Thiéblemont et al., 2024). It provides accurate 3-D velocities of GNSS receivers, which reflect the movement at the foundation of the structures on which the instruments are mounted.

Interferometric Synthetic Aperture Radar (InSAR) is another satellite-based technique that tracks the displacement of portions of the land surface that effectively reflect radar signals (e.g., Massonnet and Feigl, 1998; Bürgmann et al., 2000;

https://doi.org/10.5194/egusphere-2026-824
Preprint. Discussion started: 17 February 2026

Rosen et al., 2000; Ferretti et al., 2001; Hanssen, 2001; Torres et al., 2012). Compared to GNSS, InSAR offers broad spatial coverage, making it a potentially powerful tool. As discussed by Shirzaei et al. (2021) and Törnqvist and Blum (2024), unlike GNSS, InSAR in morphodynamically active coastal zones does not eliminate vertical accretion (or erosion) and therefore monitors surface-elevation change (SEC) rather than VLM. It has been widely applied in coastal regions globally due to its ability to capture spatial patterns of SEC (e.g., Chaussard et al., 2013; Erban et al., 2014; Higgins et al., 2014; Thiéblemont et al., 2024). In urban areas, artificial structures such as buildings act as powerful reflectors. In these settings, InSAR-derived SEC typically captures the movement of these structures, and the recorded SEC directly reflects the VLM beneath their foundation. On the other end of the spectrum, dominantly vegetated environments such as coastal wetlands pose significant challenges due to low phase coherence caused by plant growth and flooding (Zebker and Villasenor, 1992). These factors not only limit data quality but also complicate interpretation, as the observed SEC integrates both vertical accretion and subsidence, making it difficult to isolate individual processes (Törnqvist and Blum, 2024).

Despite its broad adoption, recent InSAR applications that estimate long-term SEC for a given region have revealed reproducibility challenges, as methodological differences can influence the resulting SEC maps. For example, two studies in coastal California presented substantially different results. Blackwell et al. (2020) reported generally negative SEC across the San Francisco Peninsula, with rates ranging from 0 to –2.5 mm yr^{-1}. In contrast, more recent work covering the same area (Govorcin et al., 2025) showed rates mostly near zero, including an area of slight positive SEC (uplift), plus several subsidence hot spots with rates exceeding –5 mm yr^{-1}. Govorcin et al. (2025) suggested that these discrepancies may stem from post-processing filtering and interpolation applied in Blackwell et al. (2020), which could have reduced the effective spatial resolution. Deng (2025) demonstrated similar problems in the Mississippi Delta, where three recent InSAR-based investigations show considerably divergent spatial patterns of SEC (Ohenhen et al., 2024; Wang et al., 2024; Deng, 2025).

To explore this issue further, we focus on two InSAR datasets (Ohenhen et al., 2024; Wang et al., 2024) that cover the central U.S. Gulf Coast — the region with the highest rates of projected relative sea-level (RSL) rise worldwide by 2100 (Fox-Kemper et al., 2021). This region has attracted considerable attention from the coastal subsidence research community, so the driving processes are comparatively well understood. Coastal subsidence in this area results from both long-term natural processes, such as glacial isostatic adjustment (GIA; González and Törnqvist, 2009; Love et al., 2016; Kuchar et al., 2018) and sediment compaction (Meckel et al., 2006; Chamberlain et al., 2021; Keogh et al., 2021), as well as short-term anthropogenic activity, notably fluid extraction (Morton et al., 2006; Kolker et al., 2011; Chang et al., 2014). Comparing these two InSAR studies provides an opportunity to examine how differences in methods and processing choices influence SEC spatial patterns and reported rates across different land cover types, and to assess whether the results are consistent within the reported uncertainties. We also incorporate data from independent GNSS sites to evaluate the reliability of InSAR-derived SEC rates in this coastal zone.

https://doi.org/10.5194/egusphere-2026-824
Preprint. Discussion started: 17 February 2026

2. Materials and Methods

2.1 InSAR data

The InSAR-derived SEC data in this study cover the central U.S. Gulf Coast during overlapping time periods. The first dataset (Ohenhen et al., 2024; henceforth O24), has a 50-m pixel spacing and covers the contiguous U.S. coastal zone from 2007 to 2020. O24 is based on a stochastic model that integrates InSAR line-of-sight (LOS) displacements from 2007 to 2011 and 2015 to 2020 with independent GNSS observations. The second dataset (Wang et al., 2024; henceforth W24) provides SEC data with a 1-km pixel spacing for a 4-year observation window from 2017 to 2020 for the central Texas through western Mississippi coastal zone. W24 derives SEC solely from InSAR observations, and four GNSS stations were used to calibrate relative InSAR SEC maps to the North American Plate-fixed reference frame. A Phase Reconstruction Algorithm, known as EigenSAR, was developed to mitigate severe decorrelation noise. Table 1 provides a more detailed comparison between these two datasets. In the present study, we focus only on the region where both studies overlap geographically.

Table 1. Comparison of InSAR data and processing methods between Ohenhen et al. (2024) and Wang et al. (2024).

Feature	O24	W24
Data time coverage	2007 to 2011; 2015 to 2020	2017/01 to 2020/12
Satellite(s)	Sentinel-1, ALOS-1	Sentinel-1
Spatial coverage	Contiguous U.S. coasts	Central U.S. Gulf Coast (east TX to west MS)
Core processing method	Multi-temporal InSAR processing combined with a stochastic model to integrate LOS velocities and GNSS data.	EigenSAR phase reconstruction and filtering applied to multi-looked interferograms to mitigate decorrelation noise.
Pixel spacing	50 m	1 km

To evaluate the two datasets, we first converted O24 to match the pixel spacing of W24. For each pixel in W24, we applied a circular search area with a radius of 500 m (radii between 100-400 m plus 1000 m were tested, with only minor differences) to calculate the corresponding median SEC rate in the O24 dataset (mean rates were also tested, with minimal differences). The median was chosen as a representative value because it is robust to potential outliers and better captures the central tendency regardless of the data distribution within the search area. This conversion resulted in a total of 63,153 pixels.

https://doi.org/10.5194/egusphere-2026-824
Preprint. Discussion started: 17 February 2026

The reference frame for O24 is the International GNSS Service 14 (IGS14), while W24 is referenced to the North American Plate-fixed frame (NA). However, the primary offset between IGS14 and NA occurs in the horizontal direction, and the vertical misalignment can be considered negligible.

85

https://doi.org/10.5194/egusphere-2026-824
Preprint. Discussion started: 17 February 2026

2.2 GNSS data

For the GNSS data, we expanded the study area beyond the overlapping region of the O24 and W24 coverage to better characterize background VLM along the central U.S. Gulf Coast. This expansion allows for a more robust analysis by including a larger number of sites located in the Pleistocene landscape, immediately landward of the coastal zone. The boundary was set to 95°W to 87°W and 28.5°N to 31.5°N, representing the region stretching from southeastern Texas to the westernmost portion of Florida.

Daily GNSS data and the overall vertical velocities referenced to IGS14 were downloaded from the Nevada Geodetic Laboratory (Blewitt et al., 2018, https://geodesy.unr.edu/). Vertical velocities over truncated timespans were independently estimated using the MIDAS algorithm (Blewitt et al., 2016). To ensure the reliability of these estimates, we applied the following criteria for GNSS site selection: (1) each site must have at least five years of continuous data; (2) data completeness must exceed 70%; and (3) the data must overlap with the 2007-2020 period, with at least 20% coverage within this interval.

We also compared the GNSS-derived vertical velocities referenced to NA and IGS14 frames and found them to be consistent for all GNSS sites used in this study. Similarly, GNSS velocities expressed in a regional Gulf of Mexico reference frame exhibit sub-mm yr^{-1} vertical stability (Yu and Wang, 2016), suggesting that differences in reference-frame definition introduce only minor effects on long-term vertical velocity estimates. Therefore, reference-frame choice is unlikely to affect the vertical velocity comparison in this study.

2.3 Land cover data

Land cover data were obtained from the National Land Cover Database (NLCD) (https://www.sciencebase.gov/catalog/item/664e0d2bd34e702fe8744536). We used the 2020 dataset to match the most recent time frame of the InSAR observations from the two datasets. Within the study area, 15 land cover types were identified in the NLCD. Pixels classified as open water were excluded, and the remaining 14 land cover types were grouped into five broader categories (Figure S1).

2.4 Fluid withdrawal

To identify potential anthropogenic processes that may influence GNSS vertical velocities, we examined groundwater withdrawal and the distribution of active oil and gas wells surrounding each GNSS site in the study area. For groundwater, we calculated the total volume of withdrawal within a 5 km radius centered on the GNSS site by summing yearly data (Houston et al., 2021) from 2000 to 2017. Oil and gas well information was obtained from a variety of sources, depending on the state (Figures S2 and S3).

https://doi.org/10.5194/egusphere-2026-824
Preprint. Discussion started: 17 February 2026

3. Results and Discussion

3.1 Comparison of InSAR data

The SEC rates from O24 span from −5.0 mm yr^{-1} (10^{th} percentile) to −1.7 mm yr^{-1} (90^{th} percentile), with a median of −3.0 mm yr^{-1} and a mean of -3.3 ± 1.8 mm yr^{-1} within the study area. The O24 map shows that the most negative rates occur in three distinct bowls (Figure 1a). In comparison, W24 SEC rates range from −6.2 mm yr^{-1} (10^{th} percentile) to 0.4 mm yr^{-1} (90^{th} percentile), with a median of −2.5 mm yr^{-1} and a mean of -2.8 ± 2.8 mm yr^{-1}. The W24 map includes more negative SEC bowls but they generally do not overlap with those in O24 (Figure 1b). In Louisiana's coastal wetlands, mean subsidence rates of nearly −10 mm yr^{-1}, much higher than the mean InSAR-derived rates, have been found based on a combination of surface-elevation table – marker horizon measurements and GNSS data (Nienhuis et al., 2017). This supports the notion that in wetland-dominated coastal settings, InSAR primarily captures SEC rather than VLM (i.e., subsidence) because vertical accretion offsets a substantial portion of the subsidence.

Although the summary statistics of O24 and W24 may appear broadly similar, we note that the W24 dataset has a considerably wider distribution as reflected by the larger standard deviation. A Kolmogorov-Smirnov test reveals significant distributional differences ($p<0.001$, Figure 1d), with a maximum divergence of 0.31 between their cumulative distributions (values closer to zero indicate greater similarity). In other words, the two datasets follow statistically distinct distributions, and striking spatial discrepancies persist across the region (Figure 1c).

To further investigate these differences, we performed a pixel-by-pixel comparison between O24 and W24 over the entire study area. As shown in Figure 2a, the correlation between the two datasets is weak ($R^2 = 0.05$). Nearly one-third of the pixels (28%) show an absolute SEC rate difference >3 mm yr^{-1}, and 7% show a difference >5 mm yr^{-1} (Figure 1e). We subsequently stratified the comparison by land cover categories. The correlation remains weak ($R^2 < 0.05$) for wetlands, agricultural land, and upland vegetation (Figures 2b-d). A modestly stronger correlation is observed only in developed land ($R^2 = 0.3$; Figure 2e), which increases further in medium to high developed areas ($R^2 > 0.5$; Figure 2f). In contrast, the correlation is lower in low-intensity development and open-space areas within developed land ($R^2 < 0.3$, Figure S4). These results suggest that InSAR measurements are only reasonably robust in densely urbanized settings.

https://doi.org/10.5194/egusphere-2026-824
Preprint. Discussion started: 17 February 2026

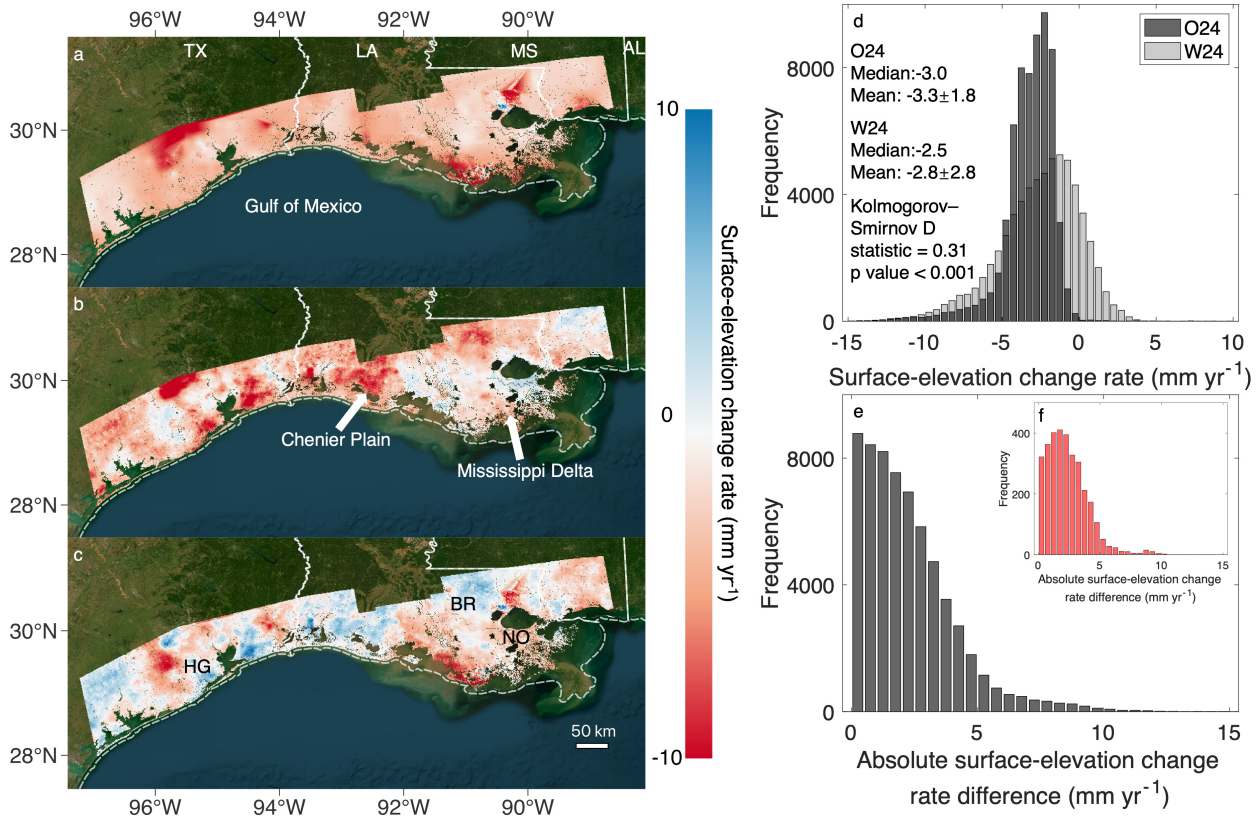

Figure 1. Maps of InSAR-derived surface-elevation change (SEC) rates and corresponding frequency histograms. (a) SEC data from the Ohenhen et al. (2024) dataset (O24), converted to match the resolution of the Wang et al. (2024) dataset (W24). TX: Texas, LA: Louisiana, MS: Mississippi, AL: Alabama; (b) SEC data from the W24 dataset; (c) SEC difference between O24 and W24. HG: Houston-Galveston area, BR: Baton Rouge, NO: New Orleans; (d) Frequency histograms and statistics of O24 and W24 SEC rates; (e) Frequency histogram of absolute SEC rate differences between O24 and W24; (f) Same as (e), but for medium to high developed land, where the impervious surface cover exceeds 50%.

https://doi.org/10.5194/egusphere-2026-824
Preprint. Discussion started: 17 February 2026

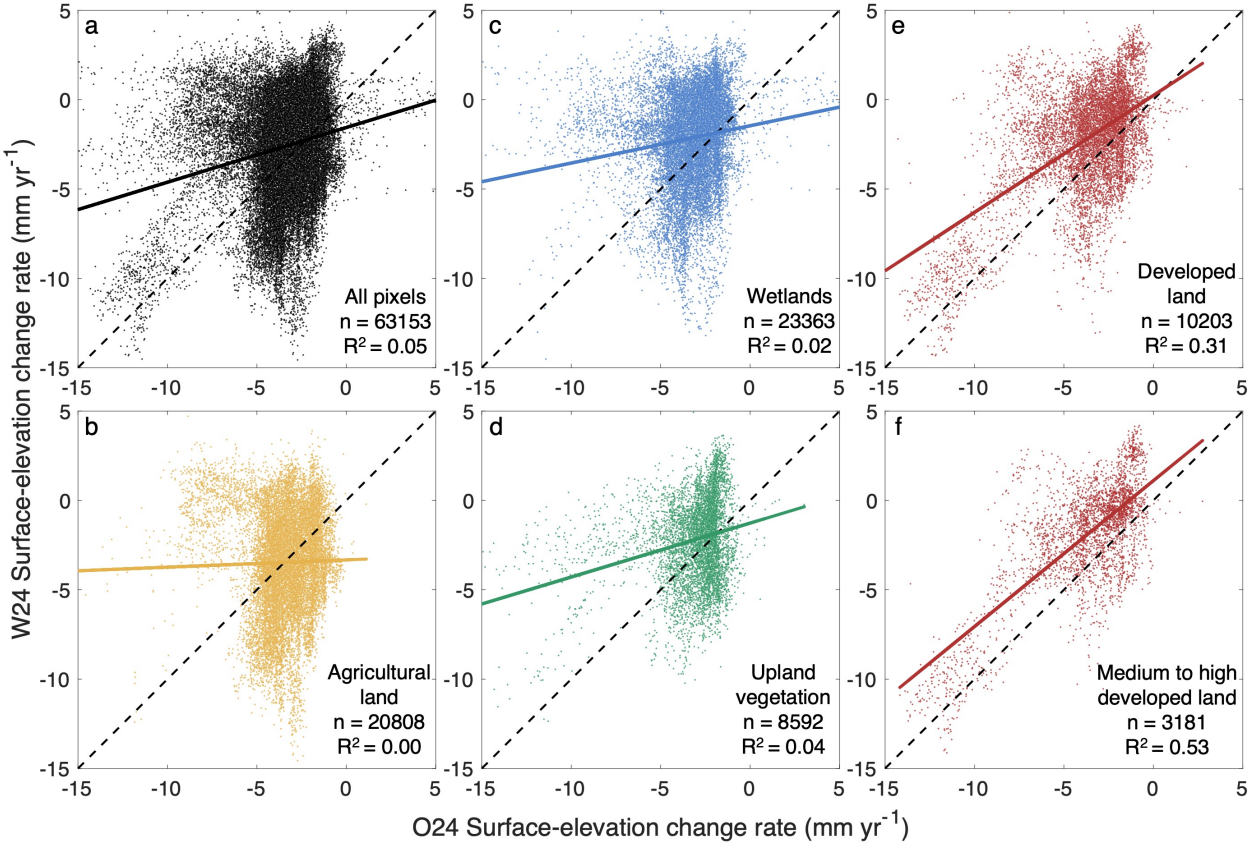

Figure 2. Pixel-by-pixel comparison of surface-elevation change (SEC) rates between the O24 (Ohenhen et al., 2024) and W24 (Wang et al., 2024) datasets. (a) All pixels; (b) Agricultural land; (c) Wetlands; (d) Upland vegetation; (e) Developed land; (f) Medium to high developed land. The thick line in each panel represents the best-fit linear regression between the two datasets. Dashed lines indicate the 1:1 reference line. The number of pixels and corresponding R^2 value are shown in the lower right corner.

https://doi.org/10.5194/egusphere-2026-824
Preprint. Discussion started: 17 February 2026

3.2 GNSS data

Applying the initial filtering criteria yielded 110 GNSS sites with a mean record length of 12.6 ± 5.0 years, from southeastern Texas to the westernmost portion of Florida. Approximately 77% of the records began after 2007, and the latest observation time was July 2024.

In Holocene depositional settings, notably coastal Louisiana, GNSS instruments only measure VLM at greater depth, given a mean foundation depth ~15 m below the land surface (Keogh and Törnqvist, 2019). In contrast, the more stable Pleistocene landscape located immediately landward of the coastal wetland zone is characterized by negligible sediment compaction or accretion. In this setting, foundation depth is not a concern and GNSS-derived VLM can be expected to be equivalent to SEC. Accordingly, we excluded GNSS sites located in Holocene deposits.

Next, we considered potential anthropogenic influence by focusing on the annual groundwater withdrawal (gallons per year) and oil and gas production (number of active wells) within a 5 km radius of each GNSS site. In the Houston-Galveston region of Texas, fluid withdrawal, particularly groundwater extraction, is a major driver of land subsidence (Braun and Ramage, 2020). The high density of active oil and gas wells (Figures S2 and S3b) suggests elevated production rates that may further contribute to subsidence in this area (Wang et al., 2024). Unlike the other states, 24 out of 30 (80%) of Texas sites have active wells (Figure S3b), indicating pervasive human influence. Therefore, all GNSS sites in Texas were excluded. These filtering steps left 41 sites situated in the Pleistocene upland along the central U.S. Gulf Coast (Figure 3a), with a mean record duration of 13.8 ± 4.8 years, a mean VLM rate of –1.3 ± 0.9 mm yr^{-1}, and a similar median rate of –1.3 mm yr^{-1} (Figure 3b).

Although we excluded sites to minimize fluid withdrawal and sediment compaction effects, some anthropogenic influence may still persist. For example, subsidence in Baton Rouge, Louisiana, is known to be significant due to groundwater pumping (Hurtado-Pulido et al., 2024). To further minimize the potential role of fluid extraction at the retained sites, we examined the annual groundwater withdrawal within a 5 km radius around each GNSS site. While no clear temporal trends were observed, several sites consistently show higher annual withdrawal and substantial cumulative extraction (Figure S5). We note that a major gap separates these high groundwater withdrawal cases from the majority of the sites, and a similar gap is observed when considering the number of active, nearby oil and gas wells (Figure S3). Accordingly, we applied an additional filter and removed five sites which may be influenced by unusually high extraction rates. The remaining 36 GNSS records, representing sites with minimal anthropogenic influence (Figure 3a) yield mean and median VLM rates of –1.1 ± 0.7 mm yr^{-1} and –1.2 mm yr^{-1}, respectively (Figure 3c). These results establish a background VLM rate that is relatively uniform across the Pleistocene landscape along the central U.S. Gulf Coast.

https://doi.org/10.5194/egusphere-2026-824
Preprint. Discussion started: 17 February 2026

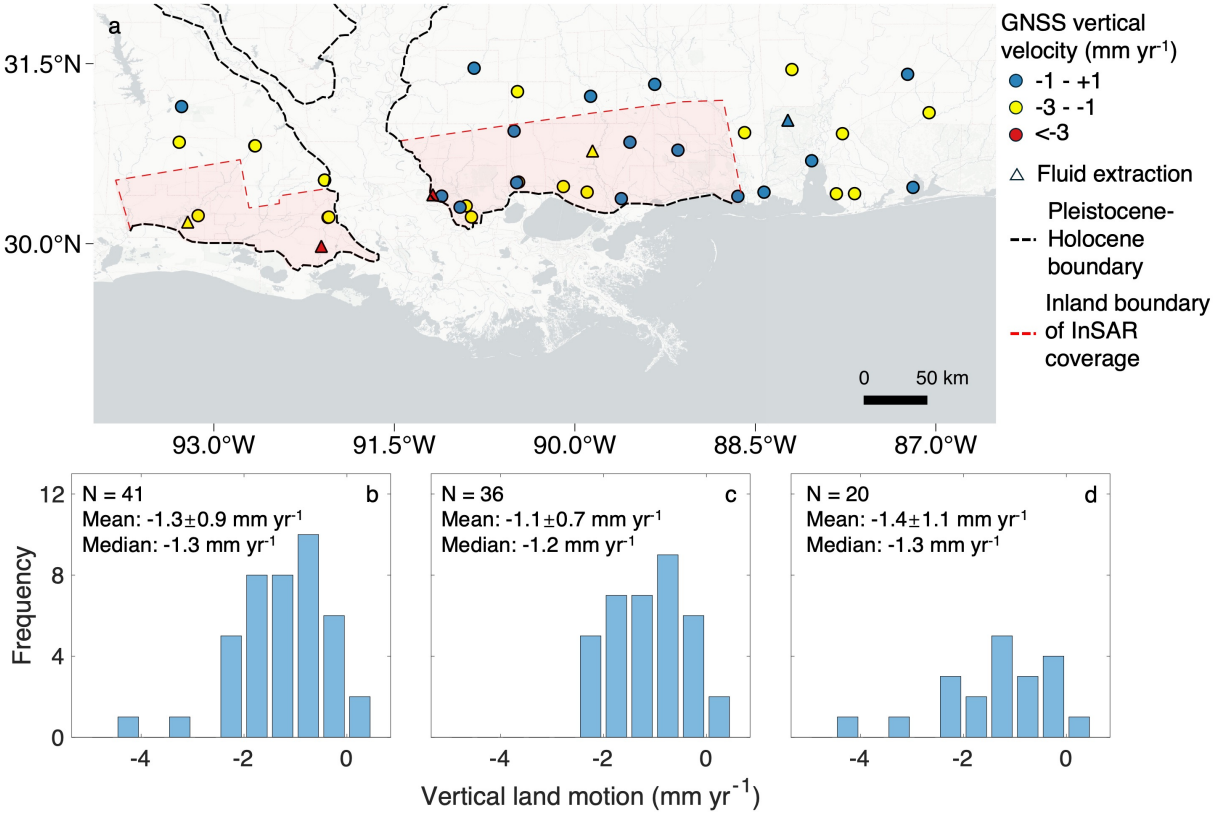

185 **Figure 3. Distribution of GNSS sites and frequency histograms of corresponding vertical land motion in the Pleistocene landscape along the central U.S. Gulf Coast. Data are provided in the Supplementary Spreadsheet. (a) Map with the GNSS sites. The Pleistocene-Holocene boundary is simplified based on the Quaternary geologic map of the Lower Mississippi Valley (Autin et al., 1991; Saucier, 1994). Frequency histograms and associated statistics are shown for (b) all 41 GNSS sites; (c) 36 GNSS sites with minimal human influence; and (d) all 20 GNSS sites within the InSAR coverage area (pink shaded area).**

190

https://doi.org/10.5194/egusphere-2026-824
Preprint. Discussion started: 17 February 2026

3.3 GNSS versus InSAR

With the background VLM rate established, a test of the InSAR datasets becomes possible: the InSAR-derived SEC rates from O24 and W24 across the Pleistocene landscape may be expected to reflect VLM and should therefore be comparable. To assess this, we focused on the portion of the Pleistocene landscape covered by both InSAR datasets, along with GNSS sites within the same region (Figure 3a). The statistics of these GNSS sites are consistent with the values reported above, with a mean rate of –1.4 ± 1.1 mm yr^{-1} and a median of –1.3 mm yr^{-1} (Figure 3d). However, SEC rates from O24 and W24 in this region show more negative mean values of –3.0 ± 1.5 mm yr^{-1} and –3.0 ± 2.6 mm yr^{-1}, respectively (Figure 4). Kolmogorov-Smirnov tests indicate maximum divergences of 0.67 for O24 (Figure 4a) and 0.47 for W24 (Figure 4b), suggesting that both InSAR-derived SEC datasets differ significantly from the GNSS-derived rates of VLM ($p < 0.001$). However, unlike the O24 dataset which is slightly offset relative to the GNSS data, the wider distribution of the W24 dataset shows better overlap, as reflected by the lower maximum divergence. The wider distribution of W24 may also capture some additional spatial variability in SEC that is not fully represented by the GNSS data.

Recognizing that InSAR captures regional signals that sparse GNSS sites might miss, we also conducted a site-level comparison to reduce potential bias from differing spatial coverage. Specifically, GNSS-derived VLM rates were compared with InSAR-derived SEC rates within varying search radii around each GNSS site (Figure S6). Across all radii, the mean O24 SEC rates (–2.0 ± 0.9 mm yr^{-1}) are consistently more negative than the mean GNSS-derived rate. At the site level, O24 and GNSS rates show a clear linear correlation ($R^2 \approx 0.3$) with low root mean square errors (RMSE < 1 mm yr^{-1}) across all search radii. A comparison using the original (50-m pixel) O24 SEC within 200 m of each GNSS site yields a similar result with significantly different distributions ($p = 0.03$). In contrast, W24 SEC rates more closely match the GNSS-derived VLM rates in terms of mean, median, and distribution, yet correlations are weaker, with RMSE values of ~1.5 mm yr^{-1} and lower R^2 values. These results suggest that neither InSAR dataset fully captures the background VLM rates over the Pleistocene landscape along the central U.S. Gulf Coast.

https://doi.org/10.5194/egusphere-2026-824
Preprint. Discussion started: 17 February 2026

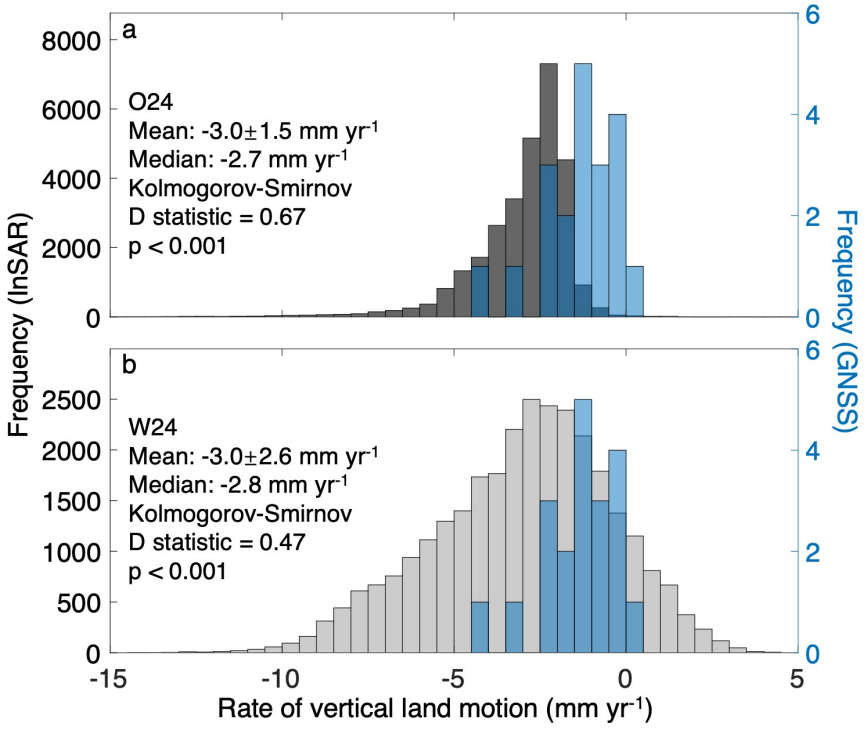

Figure 4. Comparison of InSAR and GNSS-derived vertical land motion in the Pleistocene landscape by means of frequency histograms. (a) O24 (Ohenhen et al., 2024); (b) W24 (Wang et al., 2024). GNSS sites are located within the InSAR coverage area (Figures 3a, d).

https://doi.org/10.5194/egusphere-2026-824
Preprint. Discussion started: 17 February 2026

3.4 Temporal variability

InSAR investigations over the greater New Orleans area have identified changes in local VLM rates over different time periods (Dixon et al., 2006; Jones et al., 2016; Fiaschi et al., 2025), largely attributed to changes in groundwater extraction. Therefore, the different timespans used by O24 (2007 to 2020) and W24 (2017 to 2020) could potentially contribute to the poor correlation. To explore this possibility, we focused again on the Pleistocene region and calculated VLM rates for 2007 to 2020 and 2017 to 2020, respectively, for each GNSS site using the MIDAS algorithm (Blewitt et al., 2016).

We do not observe any significant VLM rate differences between the two time periods (Figure S7). We also conducted a z-test, noting that the z-scores computed under the assumption of independence slightly underestimate the true z-scores due to the correlation between the two period estimates. Nevertheless, all 19 sites have $|z| < 1$, indicating that the two period-specific rates are consistent within the combined 1σ uncertainty. Accounting for the dependency would increase the z-scores slightly, but the differences remain statistically insignificant, confirming the robustness of the comparison. In other words, temporal variation cannot explain the poor correlation between O24 and W24.

3.5 The role of glacial isostatic adjustment

As reported above, the background VLM rate derived from GNSS sites with minimal human influence along the central U.S. Gulf Coast is in the neighborhood of –1.2 mm yr^{-1}. Since the contribution from sediment compaction and fluid withdrawal has been excluded, we focus here on other processes that may cause this subsidence rate. Faulting, which occurs mainly in discrete fault zones, is a potential mechanism contributing to observed background VLM in this region (Yuill et al., 2009; Frederick et al., 2019). However, Shen et al. (2017) estimated fault-related subsidence rates at Pleistocene sites along the central U.S. Gulf Coast to be less than –0.05 mm yr^{-1}. Furthermore, most GNSS sites used in this study are located landward of the major fault zones, ruling out faults as a major driver of the observed VLM.

The Mississippi Delta serves as the primary depocenter for sediment delivered by the Mississippi River, where Holocene sediment accumulation exceeds 100 m near the river mouth (Russell, 1936). This thick sediment load exerts pressure on the underlying lithosphere, producing downward VLM through sediment isostatic adjustment (SIA). Reported SIA rates are approximately -0.15 ± 0.07 mm yr^{-1} in central portions of the Mississippi Delta (Yu et al., 2012). However, the modeled SIA footprint with rates up to –0.3 mm yr^{-1} closer to the shoreline (Kuchar et al., 2018) indicates that most of the 36 GNSS sites analyzed here lie at the margin of the SIA-induced subsidence bowl, suggesting only a minimal contribution to the observed background VLM.

This leaves glacial isostatic adjustment (GIA) as the main factor. González and Törnqvist (2009) inferred a rate of GIA-driven subsidence of –0.6 mm yr^{-1} (or slightly less) from a late Holocene Mississippi Delta RSL record. This value is also within the range – albeit toward the lower end – of predictions for this region from global GIA models (Mitrovica and Milne, 2002; Peltier et al., 2015). GIA modeling explicitly tuned to Holocene RSL observations from the U.S. Atlantic and Gulf

https://doi.org/10.5194/egusphere-2026-824
Preprint. Discussion started: 17 February 2026

coasts (Love et al., 2016) produced results for New Orleans, Louisiana (–0.03 to –1.44 mm yr^{-1}) and Panama City, Florida (–0.09 to –1.60 mm yr^{-1}) that overlap with the rates exhibited by the GNSS data.

A regional study that modeled GIA (alongside SIA) along the central U.S. Gulf Coast produced VLM rates up to –2 mm yr^{-1}, with a best estimate in the neighborhood of –1.3 mm yr^{-1} (Wolstencroft et al., 2014), even though this value was considered to be anomalously high at the time. A subsequent study by Kuchar et al. (2018) suggested that the combined effect of GIA and SIA in this region resulted in a VLM rate of –0.8 ± 0.1 mm yr^{-1}. To further evaluate modeled versus observed background VLM rates, we examined rate differences at each GNSS site (Figures 5a, b). The agreement between site-level VLM estimates from Wolstencroft et al. (2014) and GNSS observations (Figure 5c) suggests that GIA-driven subsidence rates in this area may be about a factor of two higher than previously believed. As a result, some regional projections of long-term RSL change (Love et al., 2016) may underestimate the GIA contribution. Using a recent GIA model that incorporates lateral variation in 3-D Earth structure, Thompson et al. (2023) successfully reconciled the complex regional pattern of RSL change in North America during the Last Interglacial. Notably, estimates along the central U.S. Gulf Coast were nearly double those obtained with a 1-D Earth model, further implying that our observed background VLM could be accurate, as simpler models may underestimate the regional signal.

The question, then, is how this can be reconciled with the precise late Holocene RSL constraints. We offer two possible explanations that are not mutually exclusive. First, one component of RSL change is equatorial ocean syphoning (Mitrovica and Peltier, 1991), often assumed to be –0.2 to –0.3 mm yr^{-1} (Mitrovica and Milne, 2002). However, a more elaborate analysis of this process arrived at a wider range of –0.15 to –0.5 mm yr^{-1} (Tamisiea, 2011). Second, recent work by Creel et al. (2024) has opened the door for possible slight global sea-level fall during the late Holocene (–0.2 to –0.3 mm yr^{-1}). Collectively, there may therefore be room to close the observed gap, but more research is needed to ascertain this.

https://doi.org/10.5194/egusphere-2026-824
Preprint. Discussion started: 17 February 2026

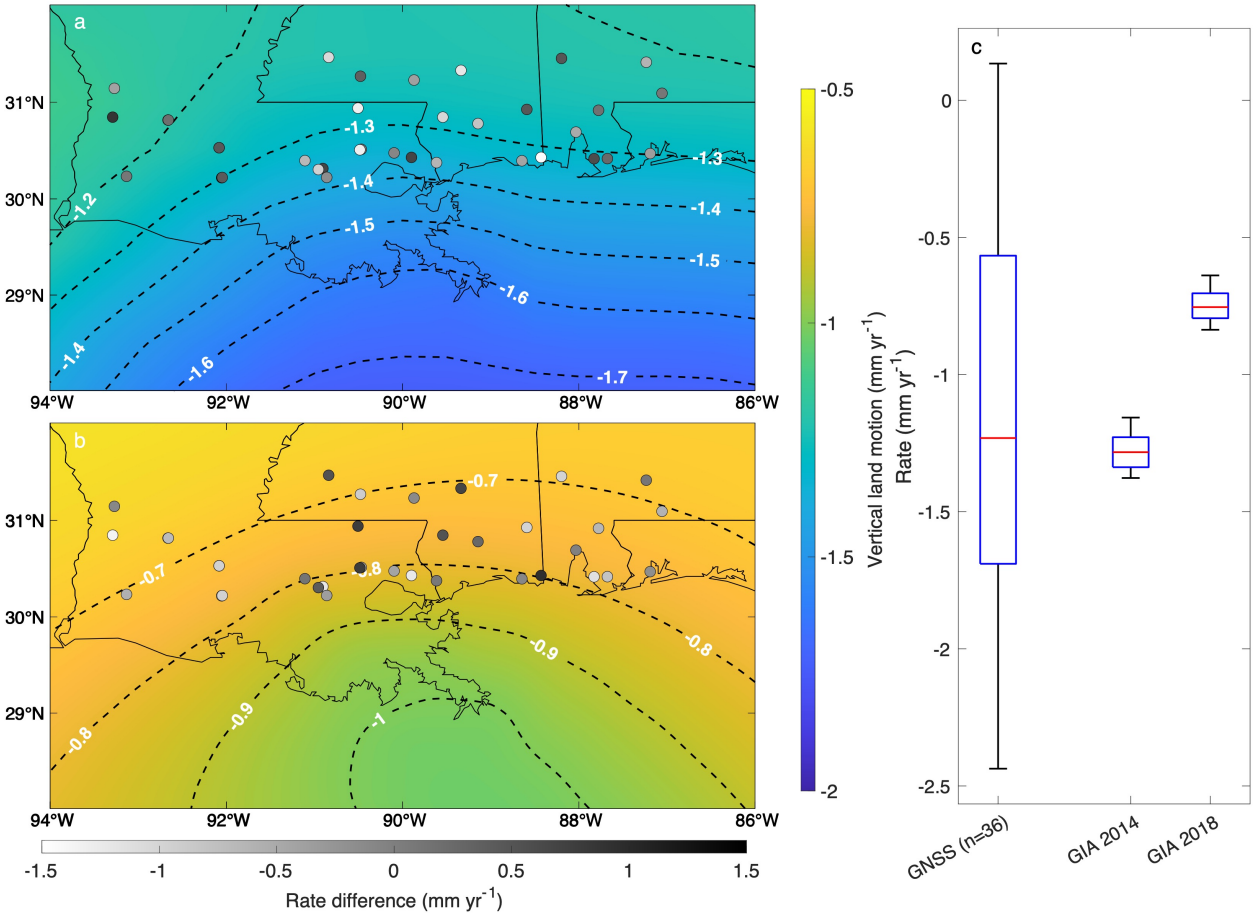

Figure 5. Modeled vertical land motion (VLM) induced by glacial isostatic adjustment (including sediment loading) and rate differences with GNSS observations along the central U.S. Gulf Coast (sites from Figure 3c). (a) VLM from Wolstencroft et al. (2014) and rate difference between GNSS-derived VLM and modeled VLM within 50 km of each GNSS site. (b) VLM from (Kuchar et al., 2018) and rate difference between GNSS-derived VLM and modeled VLM within 10 km of each GNSS site. (c) Boxplots of VLM rates from GNSS (Wolstencroft et al., 2014); GIA 2014) and (Kuchar et al., 2018); GIA 2018).

https://doi.org/10.5194/egusphere-2026-824
Preprint. Discussion started: 17 February 2026

3.6 InSAR uncertainties and future directions

With the large SEC discrepancies from InSAR reported above, we proceed to explore the potential causes. InSAR analysis over the U.S. Gulf Coast remains challenging, mainly for two reasons. First, interferograms are often corrupted by 10 cm or larger tropospheric turbulent noise (Emardson et al., 2003), while the expected rates of SEC are typically on the order of millimeters per year. Under such conditions, thousands of interferograms are required to achieve the desired millimeter-level accuracy. Second, much of the region is densely vegetated, and plant growth introduces random, unpredictable noise known as decorrelation (Zebker and Villasenor, 1992; Wang and Chen, 2022) which substantially limits the number of high-quality interferograms available for tropospheric noise mitigation. Furthermore, InSAR phase noise varies greatly among different interferograms over the same region, making inferred rates sensitive to the choice of interferogram subsets used in the analysis (Zebker and Chen, 2024).

Ohenhen et al. (2024) used 157 GNSS sites to validate the original pixel spacing (50 m) InSAR SEC map along the U.S. Gulf Coast, which yielded a standard deviation of 1.5 mm yr^{-1}. Wang et al. (2024) validated their InSAR SEC maps using VLM estimates independently collected at 183 permanent GNSS sites and six tide gauges. At 168 of the 183 GNSS sites, and at all six tide gauges, InSAR estimate errors were less than 3 mm yr^{-1} (with RMSE of ~2 mm yr^{-1}). Site-level comparisons between W24 and GNSS-derived VLM rates over the Pleistocene landscape along the central U.S. Gulf Coast (Figure S6) and over Galveston County (Dehueck, 2024; GNSS surveys were independently conducted at 11 sites by the Galveston Subsidence District) both reported RMSE values within the 3 mm yr^{-1} uncertainty range estimated in Wang et al. (2024).

Although O24 and W24 show comparable levels of uncertainty when validated against GNSS observations, significant discrepancies indicate internal inconsistencies. Differences in sensor characteristics (e.g., data fusion between L-band and C-band versus C-band only), interferometric network geometry, and coherence thresholds can each produce distinct spatial and temporal sensitivities to SEC. Processing choices, such as phase-unwrapping methods, atmospheric corrections, reference-point selection, and the approach to projecting Line-of-Sight measurements into vertical motion, further amplify these inconsistencies. In low-coherence environments such as wetlands, small variations in filtering strategies, coherence masking, or multi-looking can lead to substantial differences in resulting SEC rates. These factors highlight the importance of communicating uncertainty to stakeholders. Based on the absolute SEC differences between O24 and W24 in the medium to high developed urban area (Figure 1f, where InSAR performance is most reliable), an uncertainty of 5 mm yr^{-1} (corresponding to the 95th percentile of absolute SEC differences) is recommended for regions lacking direct ground-truthing data (e.g., areas without nearby GNSS stations).

Mitigating these discrepancies requires harmonized processing frameworks, standardized reporting of metadata and assumptions, and the integration of independent constraints (e.g., GNSS, leveling, geotechnical benchmarks, surface-elevation table – marker horizons), as emphasized by Minderhoud et al. (2025). Recent and upcoming InSAR missions have relatively short revisit cycles (6–12 days), which makes it possible to exploit the dramatic increase in SAR data volume to

https://doi.org/10.5194/egusphere-2026-824
Preprint. Discussion started: 17 February 2026

better characterize SEC as well as its uncertainties through comparing solutions derived from subsets of interferograms containing common signals of interest (Zebker et al., 2023). Future coastal InSAR products would benefit from cross-calibration exercises, shared testbeds, and open, reproducible pipelines that allow systematic comparison across datasets. Collectively, these efforts would strengthen confidence in InSAR-derived SEC estimates and reduce interpretational uncertainty in coastal lowland environments. Moving forward, continued collaboration and systematic engagement within the InSAR community will be essential to further reduce uncertainties and improve the reliability of SEC measurements.

https://doi.org/10.5194/egusphere-2026-824
Preprint. Discussion started: 17 February 2026

4. Conclusions

We show that two recent InSAR datasets from the central U.S. Gulf Coast, obtained by means of different methods, exhibit negligible spatial correlation ($R^2 = 0.05$), despite producing comparable mean SEC rates. Correlation improves notably ($R^2 > 0.5$) in medium to highly developed areas, reflecting the better coherence and more stable scattering condition in built environments, but InSAR struggles in densely vegetated environments. Independent GNSS records from Pleistocene landscapes where shallow subsidence and sediment accretion are minimal, indicate a median background VLM of about –1.2 mm yr^{-1}, but neither InSAR dataset can reproduce this signal. The comparison highlights the importance of integrating GNSS and other ground-based constraints when evaluating regional InSAR-derived SEC patterns. Caution is therefore warranted when interpreting rates <5 mm yr^{-1} from InSAR-derived maps of low-elevation coastal zones, especially when they are used to inform policy or management decisions. This underscores the need for harmonized processing frameworks, transparent methodological documentation, and systematic cross-validation to ensure robust interpretation of InSAR products in densely vegetated environments.

Our GNSS analysis further reveals that the background VLM along the central U.S. Gulf Coast is just over –1 mm yr^{-1}, primarily driven by GIA. This is roughly double the previously inferred rate, indicating that GIA may have been underestimated in this region. This suggests that regional projections of long-term RSL change may have underestimated the GIA contribution. Updating these projections, together with re-evaluating the total subsidence budget along the central U.S. Gulf Coast, would improve hazard assessment and adaptation planning. The GNSS-derived background VLM rate presented here provides a benchmark for future refinement of regional GIA models and offers an important reference for calibrating InSAR-based subsidence assessments.

https://doi.org/10.5194/egusphere-2026-824
Preprint. Discussion started: 17 February 2026

Data availability

GNSS data discussed in this study are available in the Data Set S1.

Author contributions

GL and TET conceptualized the study. TET supervised the project. GL and TET developed the methodology. GL performed the formal analysis and visualization. GL, TET, and JC conducted the investigation. GL and TET prepared the original draft. GL, TET, and JC reviewed and edited the manuscript.

Competing interests

The authors declare no conflicts of interest relevant to this study.

Disclaimer

Copernicus Publications remains neutral with regard to jurisdictional claims made in the text, published maps, institutional affiliations, or any other geographical representation in this paper. While Copernicus Publications makes every effort to include appropriate place names, the final responsibility lies with the authors. Views expressed in the text are those of the authors and do not necessarily reflect the views of the publisher.

Acknowledgements

G. Li acknowledges support from the Vokes Fellowship at Tulane University. This research was also supported in part by the Louisiana Board of Regents Endowed Professorships subprogram. We thank Manoochehr Shirzaei for comments and insights that improved this manuscript. We thank Sönke Dangendorf, Cathleen Jones, and Philip Minderhoud for valuable feedback and constructive exchanges. We also thank Glenn Milne and Martin Wolstencroft for insights on glacial isostatic adjustment and for providing data, and Geoffrey Blewitt for clarification and guidance on GNSS analysis and for developing and maintaining the GNSS data repository used here.

https://doi.org/10.5194/egusphere-2026-824
Preprint. Discussion started: 17 February 2026

References

Autin, W. J., Burns, S. F., Miller, B. J., Saucier, R. T., and Snead, J. I.: Quaternary Geology of the Lower Mississippi Valley, in: Quaternary Nonglacial Geology: Conterminous U.S., edited by: Morrison, R. B., Geological Society of America, Plate 6, https://doi.org/10.1130/DNAG-GNA-K2.547, 1991.

Bijlsma, L., Ehler, C. N., Klein, R. J. T., Kulshrestha, S. M., McLean, R. F., Mimura, N., Nicholls, R. J., Nurse, L. A., Perez Nieto, H., Stakhiv, E. Z., Turner, R. K., and Warrick, R. A.: Coastal Zones and Small Islands, in: Climate Change 1995: Impacts, Adaptations and Mitigation of Climate Change: Scientific-Technical Analyses, edited by: Watson, R. T., Zinyowera, M. C., and Moss, R. H., Cambridge University Press, Cambridge, United Kingdom, 289-324, 1996.

Blackwell, E., Shirzaei, M., Ojha, C., and Werth, S.: Tracking California's sinking coast from space: Implications for relative sea-level rise, Science Advances, 6, eaba4551, https://doi.org/10.1126/sciadv.aba4551, 2020.

Blewitt, G., Hammond, W., and Kreemer, C.: Harnessing the GPS data explosion for interdisciplinary science, Eos, 99, https://doi.org/10.1029/2018eo104623, 2018.

Blewitt, G., Kreemer, C., Hammond, W. C., and Gazeaux, J.: MIDAS robust trend estimator for accurate GPS station velocities without step detection, Journal of Geophysical Research: Solid Earth, 121, 2054-2068, https://doi.org/10.1002/2015JB012552, 2016.

Bouin, M.-N. and Wöppelmann, G.: Land motion estimates from GPS at tide gauges: a geophysical evaluation, Geophysical Journal International, 180, 193-209, https://doi.org/10.1111/j.1365-246X.2009.04411.x, 2010.

Braun, C. L. and Ramage, J. K.: Status of groundwater-level altitudes and long-term groundwater-level changes in the Chicot, Evangeline, and Jasper aquifers, Houston-Galveston region, Texas, 2020, U.S. Geological Survey Scientific Investigations Report 2020–5089, 18 pp., https://doi.org/10.3133/sir20205089, 2020.

Bürgmann, R., Rosen, P. A., and Fielding, E. J.: Synthetic aperture radar interferometry to measure Earth's surface topography and its deformation, Annu. Rev. Earth Planet. Sci., 28, 169-209, https://doi.org/10.1146/annurev.earth.28.1.169, 2000.

Chamberlain, E., Shen, Z., Kim, W., McKinley, S., Anderson, S., and Törnqvist, T.: Does load-induced shallow subsidence inhibit delta growth?, Journal of Geophysical Research: Earth Surface, 126, e2021JF006153, https://doi.org/10.1029/2021JF006153, 2021.

Chang, C., Mallman, E., and Zoback, M.: Time-dependent subsidence associated with drainage-induced compaction in Gulf of Mexico shales bounding a severely depleted gas reservoir, AAPG Bulletin, 98, 1145-1159, https://doi.org/10.1306/11111313009, 2014.

Chaussard, E., Amelung, F., Abidin, H., and Hong, S.-H.: Sinking cities in Indonesia: ALOS PALSAR detects rapid subsidence due to groundwater and gas extraction, Remote Sensing of Environment, 128, 150-161, https://doi.org/10.1016/j.rse.2012.10.015, 2013.

Creel, R. C., Austermann, J., Kopp, R. E., Khan, N. S., Albrecht, T., and Kingslake, J.: Global mean sea level likely higher than present during the holocene, Nature Communications, 15, 10731, https://doi.org/10.1038/s41467-024-54535-0, 2024.

deHueck, N.: Untangling the causes of InSAR-derived land subsidence in Galveston County, Texas, The University of Texas at Austin, Austin, TX, 2024.

Deng, F.: Current Subsidence Rates of the Mississippi River Delta from Satellite InSAR: Onshore and Offshore, Earth and Space Science, 12, e2025EA004252, https://doi.org/10.1029/2025EA004252, 2025.

Dixon, T. H.: An introduction to the Global Positioning System and some geological applications, Reviews of Geophysics, 29, 249-276, https://doi.org/10.1029/91RG00152, 1991.

Dixon, T. H., Amelung, F., Ferretti, A., Novali, F., Rocca, F., Dokka, R., Sella, G., Kim, S.-W., Wdowinski, S., and Whitman, D.: Subsidence and flooding in New Orleans, Nature, 441, 587-588, https://doi.org/10.1038/441587a, 2006.

Emardson, T., Simons, M., and Webb, F.: Neutral atmospheric delay in interferometric synthetic aperture radar applications: Statistical description and mitigation, Journal of Geophysical Research: Solid Earth, 108, 2231, https://doi.org/10.1029/2002JB001781, 2003.

Erban, L. E., Gorelick, S. M., and Zebker, H. A.: Groundwater extraction, land subsidence, and sea-level rise in the Mekong Delta, Vietnam, Environmental Research Letters, 9, 084010, https://doi.org/10.1088/1748-9326/9/8/084010, 2014.

Ferretti, A., Prati, C., and Rocca, F.: Permanent scatterers in SAR interferometry, IEEE Transactions on Geoscience and Remote Sensing, 39, 8-20, https://doi.org/10.1109/36.898661, 2001.

https://doi.org/10.5194/egusphere-2026-824
Preprint. Discussion started: 17 February 2026

Fiaschi, S., Allison, M. A., and Jones, C. E.: Vertical land motion in Greater New Orleans: Insights into underlying drivers and impact to flood protection infrastructure, Science Advances, 11, eadt5046, https://doi.org/10.1126/sciadv.adt5046, 2025.

Fox-Kemper, B., Hewitt, H. T., Xiao, C., Aðalgeirsdóttir, G., Drijfhout, S. S., Edwards, T. L., Golledge, N. R., Hemer, M., Kopp, R. E., Krinner, G., Mix, A., Notz, D., Nowicki, S., Nurhati, I. S., Ruiz, L., Sallée, J.-B., Slangen, A. B. A., and Yu, Y.: Ocean, Cryosphere and Sea Level Change, in: Climate Change 2021: The Physical Science Basis, edited by: Masson-Delmotte, V., Zhai, P., Pirani, A., Connors, S. L., Péan, C., Berger, S., Caud, N., Chen, Y., Goldfarb, L., Gomis, M. I., Huang, M., Leitzell, K., Lonnoy, E., Matthews, J. B. R., Maycock, T. K., Waterfield, T., Yelekçi, O., Yu, R., and Zhou, B., Cambridge University Press, Cambridge, United Kingdom and New York, NY, USA, 1211–1362, https://doi.org/10.1017/9781009157896.011, 2021.

Frederick, B. C., Blum, M., Fillon, R., and Roberts, H.: Resolving the contributing factors to Mississippi Delta subsidence: Past and Present, Basin Research, 31, 171-190, https://doi.org/10.1111/bre.12314, 2019.

González, J. L. and Törnqvist, T. E.: A new Late Holocene sea-level record from the Mississippi Delta: evidence for a climate/sea level connection?, Quaternary Science Reviews, 28, 1737-1749, https://doi.org/10.1016/j.quascirev.2009.04.003, 2009.

Govorcin, M., Bekaert, D. P., Hamlington, B. D., Sangha, S. S., and Sweet, W.: Variable vertical land motion and its impacts on sea level rise projections, Science Advances, 11, eads8163, https://doi.org/10.1126/sciadv.ads8163, 2025.

Hammond, W. C., Blewitt, G., Kreemer, C., and Nerem, R. S.: GPS imaging of global vertical land motion for studies of sea level rise, Journal of Geophysical Research: Solid Earth, 126, e2021JB022355, https://doi.org/10.1029/2021JB022355, 2021.

Hanssen, R. F.: Radar Interferometry: Data Interpretation and Error Analysis, 1, Remote Sensing and Digital Image Processing, Springer Dordrecht, https://doi.org/10.1007/0-306-47633-9, 2001.

Hauer, M. E., Fussell, E., Mueller, V., Burkett, M., Call, M., Abel, K., McLeman, R., and Wrathall, D.: Sea-level rise and human migration, Nature Reviews Earth & Environment, 1, 28-39, https://doi.org/10.1038/s43017-019-0002-9, 2020.

Higgins, S. A., Overeem, I., Steckler, M. S., Syvitski, J. P., Seeber, L., and Akhter, S. H.: InSAR measurements of compaction and subsidence in the Ganges-Brahmaputra Delta, Bangladesh, Journal of Geophysical Research: Earth Surface, 119, 1768-1781, https://doi.org/10.1002/2014JF003117, 2014.

Houston, N., Wallace, D., Robinson, A., and Foster, L.: Groundwater-withdrawal data from the coastal lowlands aquifer system in parts of Texas Louisiana Mississippi Alabama and Florida 1925-2018, US Geological Survey. https://doi.org/10.5066/P9L2UXSI, 2021.

Hurtado-Pulido, C., Amer, R., Ebinger, C., and Holcomb, H.: Variations in subsidence patterns in the Gulf of Mexico passive margin from airborne-LiDAR data and time series InSAR: Baton Rouge case study, Journal of Geophysical Research: Earth Surface, 129, e2023JF007406, https://doi.org/10.1029/2023JF007406, 2024.

Jones, C. E., An, K., Blom, R. G., Kent, J. D., Ivins, E. R., and Bekaert, D.: Anthropogenic and geologic influences on subsidence in the vicinity of New Orleans, Louisiana, Journal of Geophysical Research: Solid Earth, 121, 3867-3887, https://doi.org/10.1002/2015JB012636, 2016.

Keogh, M. E. and Törnqvist, T. E.: Measuring rates of present-day relative sea-level rise in low-elevation coastal zones: a critical evaluation, Ocean Science, 15, 61-73, https://doi.org/10.5194/os-15-61-2019, 2019.

Keogh, M. E., Törnqvist, T. E., Kolker, A. S., Erkens, G., and Bridgeman, J. G.: Organic matter accretion, shallow subsidence, and river delta sustainability, Journal of Geophysical Research: Earth Surface, 126, e2021JF006231, https://doi.org/10.1029/2021JF006231, 2021.

Kolker, A. S., Allison, M. A., and Hameed, S.: An evaluation of subsidence rates and sea-level variability in the northern Gulf of Mexico, Geophysical Research Letters, 38, L21404, https://doi.org/10.1029/2011GL049458, 2011.

Kuchar, J., Milne, G., Wolstencroft, M., Love, R., Tarasov, L., and Hijma, M.: The influence of sediment isostatic adjustment on sea level change and land motion along the US Gulf Coast, Journal of Geophysical Research: Solid Earth, 123, 780-796, https://doi.org/10.1002/2017JB014695, 2018.

Love, R., Milne, G. A., Tarasov, L., Engelhart, S. E., Hijma, M. P., Latychev, K., Horton, B. P., and Törnqvist, T. E.: The contribution of glacial isostatic adjustment to projections of sea-level change along the Atlantic and Gulf coasts of North America, Earth's Future, 4, 440-464, https://doi.org/10.1002/2016EF000363, 2016.

Massonnet, D. and Feigl, K. L.: Radar interferometry and its application to changes in the Earth's surface, Reviews of Geophysics, 36, 441-500, https://doi.org/10.1029/97RG03139, 1998.

https://doi.org/10.5194/egusphere-2026-824
Preprint. Discussion started: 17 February 2026

Mcclusky, S., Balassanian, S., Barka, A., Demir, C., Ergintav, S., Georgiev, I., Gurkan, O., Hamburger, M., Hurst, K., and Kahle, H.: Global Positioning System constraints on plate kinematics and dynamics in the eastern Mediterranean and Caucasus, Journal of Geophysical Research: Solid Earth, 105, 5695-5719, https://doi.org/10.1029/1999JB900351, 2000.

Meckel, T., ten Brink, U. S., and Williams, S. J.: Current subsidence rates due to compaction of Holocene sediments in southern Louisiana, Geophysical Research Letters, 33, L11403, https://doi.org/10.1029/2006GL026300, 2006.

Milliman, J. D. and Haq, B. U.: Sea-level rise and coastal subsidence: Causes, consequences, and strategies, 1, Coastal Systems and Continental Margins, Springer Dordrecht, https://doi.org/10.1007/978-94-015-8719-8, 1996.

Minderhoud, P., Shirzaei, M., and Teatini, P.: From InSAR-derived subsidence to relative sea-level rise—A call for rigor, Earth's Future, 13, e2024EF005539, https://doi.org/10.1029/2024EF005539, 2025.

Mitrovica, J. and Milne, G.: On the origin of late Holocene sea-level highstands within equatorial ocean basins, Quaternary Science Reviews, 21, 2179-2190, https://doi.org/10.1016/S0277-3791(02)00080-X, 2002.

Mitrovica, J. X. and Peltier, W. R.: On postglacial geoid subsidence over the equatorial oceans, Journal of Geophysical Research: Solid Earth, 96, 20053-20071, https://doi.org/10.1029/91JB01284, 1991.

Morton, R. A., Bernier, J. C., and Barras, J. A.: Evidence of regional subsidence and associated interior wetland loss induced by hydrocarbon production, Gulf Coast region, USA, Environmental Geology, 50, 261-274, https://doi.org/10.1007/s00254-006-0207-3, 2006.

Nienhuis, J. H., Törnqvist, T. E., Jankowski, K. L., Fernandes, A. M., and Keogh, M. E.: A new subsidence map for coastal Louisiana, GSA Today, 27, 58-59, https://doi.org/10.1130/GSATG337GW, 2017.

Ohenhen, L. O., Shirzaei, M., Ojha, C., Sherpa, S. F., and Nicholls, R. J.: Disappearing cities on US coasts, Nature, 627, 108-115, https://doi.org/10.1038/s41586-024-07038-3, 2024.

Peltier, W. R., Argus, D., and Drummond, R.: Space geodesy constrains ice age terminal deglaciation: The global ICE-6G_C (VM5a) model, Journal of Geophysical Research: Solid Earth, 120, 450-487, https://doi.org/10.1002/2014JB011176, 2015.

Rosen, P. A., Hensley, S., Joughin, I. R., Li, F. K., Madsen, S. N., Rodriguez, E., and Goldstein, R. M.: Synthetic aperture radar interferometry, Proceedings of the IEEE, 88, 333-382, https://doi.org/10.1109/5.838084, 2000.

Russell, R. J.: Physiography of Lower Mississippi River Delta, in: Lower Mississippi River Delta, Reports on the Geology of Plaquemines and St. Bernard Parishes, Geological Bulletin No. 8, Department of Conservation, Louisiana Geological Survey, New Orleans, LA, 3–199, 1936.

Saucier, R. T.: Geomorphology and Quaternary Geologic History of the Lower Mississippi Valley, U.S. Army Corps of Engineers, Waterways Experiment Station, Vicksburg, MS, 1994.

Segall, P. and Davis, J. L.: GPS applications for geodynamics and earthquake studies, Annu. Rev. Earth Planet. Sci., 25, 301-336, https://doi.org/10.1146/annurev.earth.25.1.301, 1997.

Sella, G. F., Dixon, T. H., and Mao, A.: REVEL: A model for recent plate velocities from space geodesy, Journal of Geophysical Research: Solid Earth, 107, 2081, https://doi.org/10.1029/2000JB000033, 2002.

Sella, G. F., Stein, S., Dixon, T. H., Craymer, M., James, T. S., Mazzotti, S., and Dokka, R. K.: Observation of glacial isostatic adjustment in "stable" North America with GPS, Geophysical Research Letters, 34, L02306, https://doi.org/10.1029/2006GL027081, 2007.

Shen, Z., Dawers, N. H., Törnqvist, T. E., Gasparini, N. M., Hijma, M. P., and Mauz, B.: Mechanisms of late Quaternary fault throw-rate variability along the north central Gulf of Mexico coast: Implications for coastal subsidence, Basin Research, 29, 557-570, https://doi.org/10.1111/bre.12184, 2017.

Shirzaei, M., Freymueller, J., Törnqvist, T. E., Galloway, D. L., Dura, T., and Minderhoud, P. S.: Measuring, modelling and projecting coastal land subsidence, Nature Reviews Earth & Environment, 2, 40-58, https://doi.org/10.1038/s43017-020-00115-x, 2021.

Tamisiea, M. E.: Ongoing glacial isostatic contributions to observations of sea level change, Geophysical Journal International, 186, 1036-1044, https://doi.org/10.1111/j.1365-246X.2011.05116.x, 2011.

Thiéblemont, R., Le Cozannet, G., Nicholls, R. J., Rohmer, J., Wöppelmann, G., Raucoules, D., de Michele, M., Toimil, A., and Lincke, D.: Assessing current coastal subsidence at continental scale: Insights from Europe using the European Ground Motion Service, Earth's Future, 12, e2024EF004523, https://doi.org/10.1029/2024EF004523, 2024.

Thompson, S. B., Creveling, J. R., Latychev, K., and Mitrovica, J. X.: Three-dimensional glacial isostatic adjustment modeling reconciles conflicting geographic trends in North American marine isotope stage 5a relative sea level observations, Geology, 51, 808-812, https://doi.org/10.1130/G51257.1, 2023.

https://doi.org/10.5194/egusphere-2026-824
Preprint. Discussion started: 17 February 2026

Törnqvist, T. E. and Blum, M. D.: What is coastal subsidence?, Cambridge Prisms: Coastal Futures, 2, e2, https://doi.org/10.1017/cft.2024.1, 2024.
Torres, R., Snoeij, P., Geudtner, D., Bibby, D., Davidson, M., Attema, E., Potin, P., Rommen, B., Floury, N., and Brown, M.: GMES Sentinel-1 mission, Remote Sensing of Environment, 120, 9-24, https://doi.org/10.1016/j.rse.2011.05.028, 2012.
Wang, K. and Chen, J.: Accurate persistent scatterer identification based on phase similarity of radar pixels, IEEE Transactions on Geoscience and Remote Sensing, 60, 1-13, https://doi.org/10.1109/TGRS.2022.3210868, 2022.
Wang, K., Chen, J., Valseth, E., Wells, G., Bettadpur, S., Jones, C. E., and Dawson, C.: Subtle land subsidence elevates future storm surge risks along the Gulf Coast of the United States, Journal of Geophysical Research: Earth Surface, 129, e2024JF007858, https://doi.org/10.1029/2024JF007858, 2024.
Wolstencroft, M., Shen, Z., Törnqvist, T. E., Milne, G. A., and Kulp, M.: Understanding subsidence in the Mississippi Delta region due to sediment, ice, and ocean loading: Insights from geophysical modeling, Journal of Geophysical Research: Solid Earth, 119, 3838-3856, https://doi.org/10.1002/2013JB010928, 2014.
Yu, J. and Wang, G.: GPS-derived ground deformation (2005–2014) within the Gulf of Mexico region referred to a stable Gulf of Mexico reference frame, Natural Hazards and Earth System Sciences, 16, 1583-1602, https://doi.org/10.5194/nhess-16-1583-2016, 2016.
Yu, S.-Y., Törnqvist, T. E., and Hu, P.: Quantifying Holocene lithospheric subsidence rates underneath the Mississippi Delta, Earth and Planetary Science Letters, 331, 21-30, https://doi.org/10.1016/j.epsl.2012.02.021, 2012.
Yuill, B., Lavoie, D., and Reed, D. J.: Understanding subsidence processes in coastal Louisiana, Journal of Coastal Research, 23-36, https://doi.org/10.2112/SI54-012.1, 2009.
Zebker, H. A. and Villasenor, J.: Decorrelation in interferometric radar echoes, IEEE Transactions on Geoscience and Remote Sensing, 30, 950-959, https://doi.org/10.1109/36.175330, 1992.
Zebker, M. S. and Chen, J.: A robust method for selecting a high-quality interferogram subset in InSAR surface deformation analysis, Geophysical Research Letters, 51, e2024GL111339, https://doi.org/10.1029/2024GL111339, 2024.
Zebker, M. S., Chen, J., and Hesse, M. A.: Robust surface deformation and tropospheric noise characterization from common-reference interferogram subsets, IEEE Transactions on Geoscience and Remote Sensing, 61, 1-14, https://doi.org/10.1109/TGRS.2023.3288019, 2023.